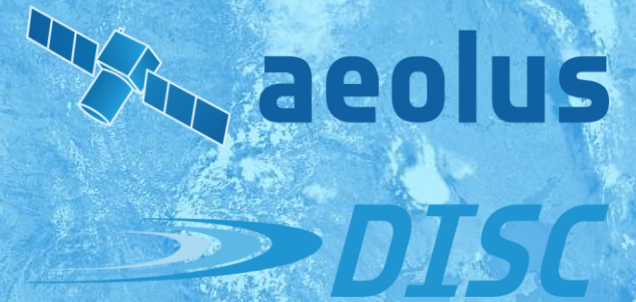




31ST INTERNATIONAL LASER RADAR CONFERENCE
22ND COHERENT LASER RADAR CONFERENCE
LANDSHUT, GERMANY, 23-28 JUNE 2024



PERFORMANCE OF THE LASER TRANSMITTERS AND RECEIVER SIGNAL EVOLUTION DURING THE AEOLUS MISSION FROM 2018 TO 2023

**Oliver Lux¹, Christian Lemmerz¹, Karsten Schmidt², Valeria De Sanctis³, Paolo Bravetti⁴,
Denny Wernham⁵, Trismono Candra Krisna⁵, Tommaso Parrinello⁶, and Oliver Reitebuch¹**

¹ Deutsches Zentrum für Luft- und Raumfahrt (DLR), Institute of Atmospheric Physics, Münchener Str. 20, 82234 Oberpfaffenhofen, Germany

² Deutsches Zentrum für Luft- und Raumfahrt (DLR), Remote Sensing Technology Institute, Kalkhorstweg 53, 17235 Neustrelitz, Germany

³ Leonardo S.p.A., Via Industria, 4, 00040 Pomezia RM, Italy

⁴ Airbus Italia S.p.A., Via dei Luxardo, 22-24, 00156 Rome, Italy

⁵ European Space Agency, European Space Research and Technology Centre (ESTEC), Keplerlaan 1, Noordwijk, NL-2201AZ, The Netherlands

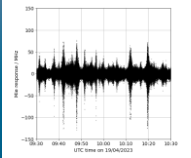
⁶ European Space Agency, European Space Research Institute (ESRIN), Largo Galileo Galilei, 1, 00044 Frascati RM, Italy



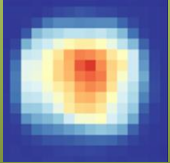
AIRBUS



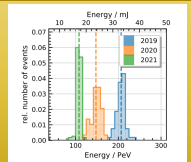
OUTLINE



Performance of the ALADIN laser transmitters



Receiver signal evolution



Measurements at the Pierre Auger Observatory

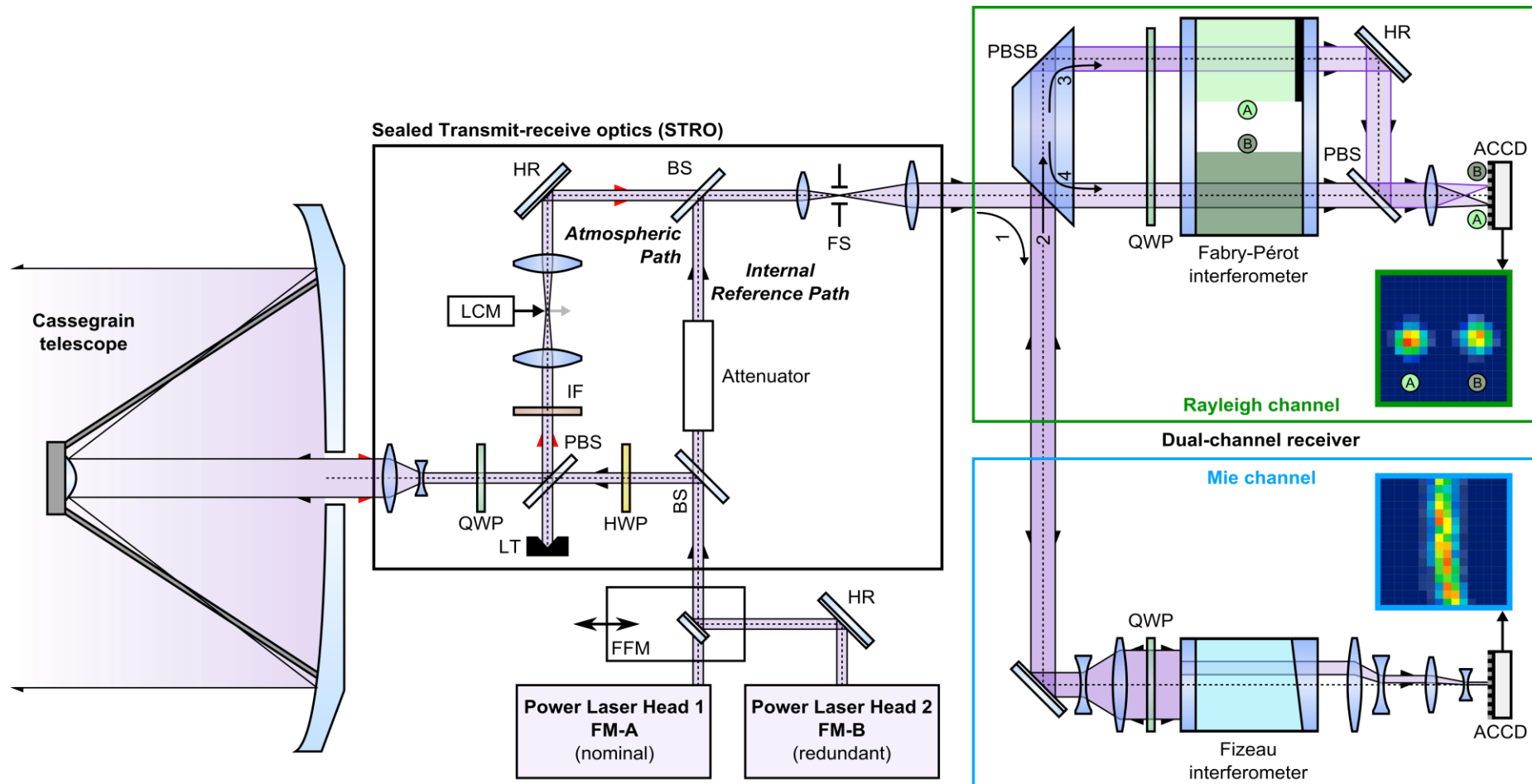


**PERFORMANCE OF THE
ALADIN LASER TRANSMITTERS**

ALADIN instrument design



- **First Doppler wind lidar in space** consisting of UV laser transmitter, 1.5 m telescope and dual-channel receiver
- **Complementary Rayleigh and Mie channels** for sensing the Doppler shift from molecules and particles (aerosols, clouds)
- **Measurement of the Doppler frequency shift with accuracy of 10^{-8}** in order to achieve wind speed accuracy of 1 m/s



Doppler equation:

$$\Delta f = 2f_0 \frac{v_{LOS}}{c}$$

relative Doppler shift:

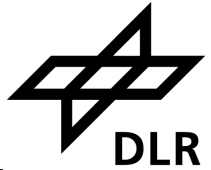
$$\Delta f / f_0 \approx 10^{-8}$$

1 m/s (Line-of-sight)
 $\sim 5.64 \text{ MHz} \sim 2.37 \text{ fm}$

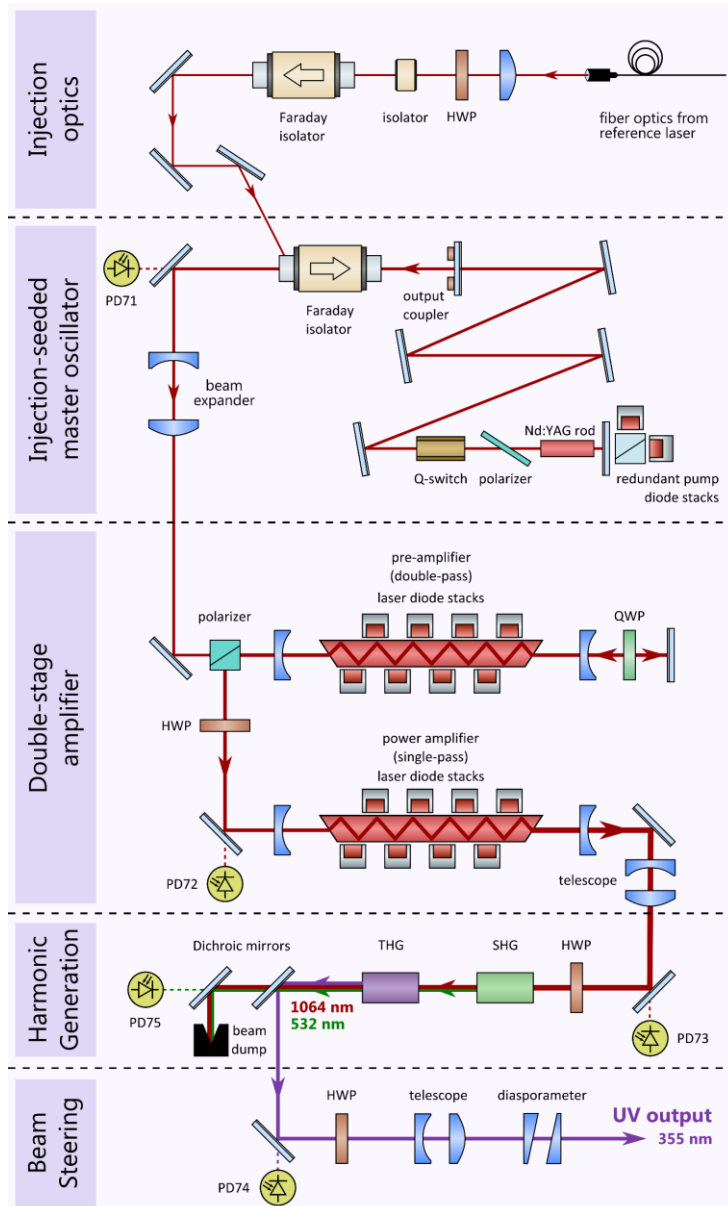


Laser design and specifications

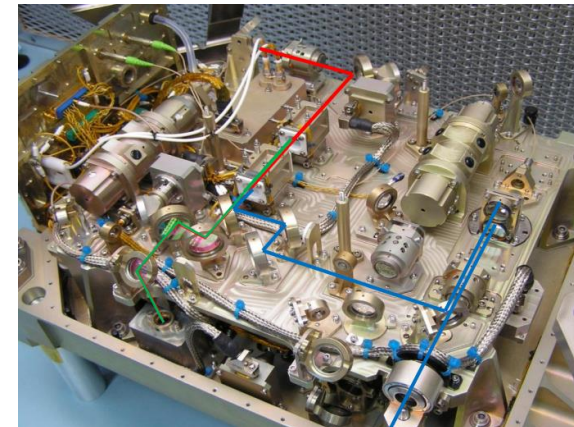
Lux et al., in preparation



AIRBUS LEONARDO

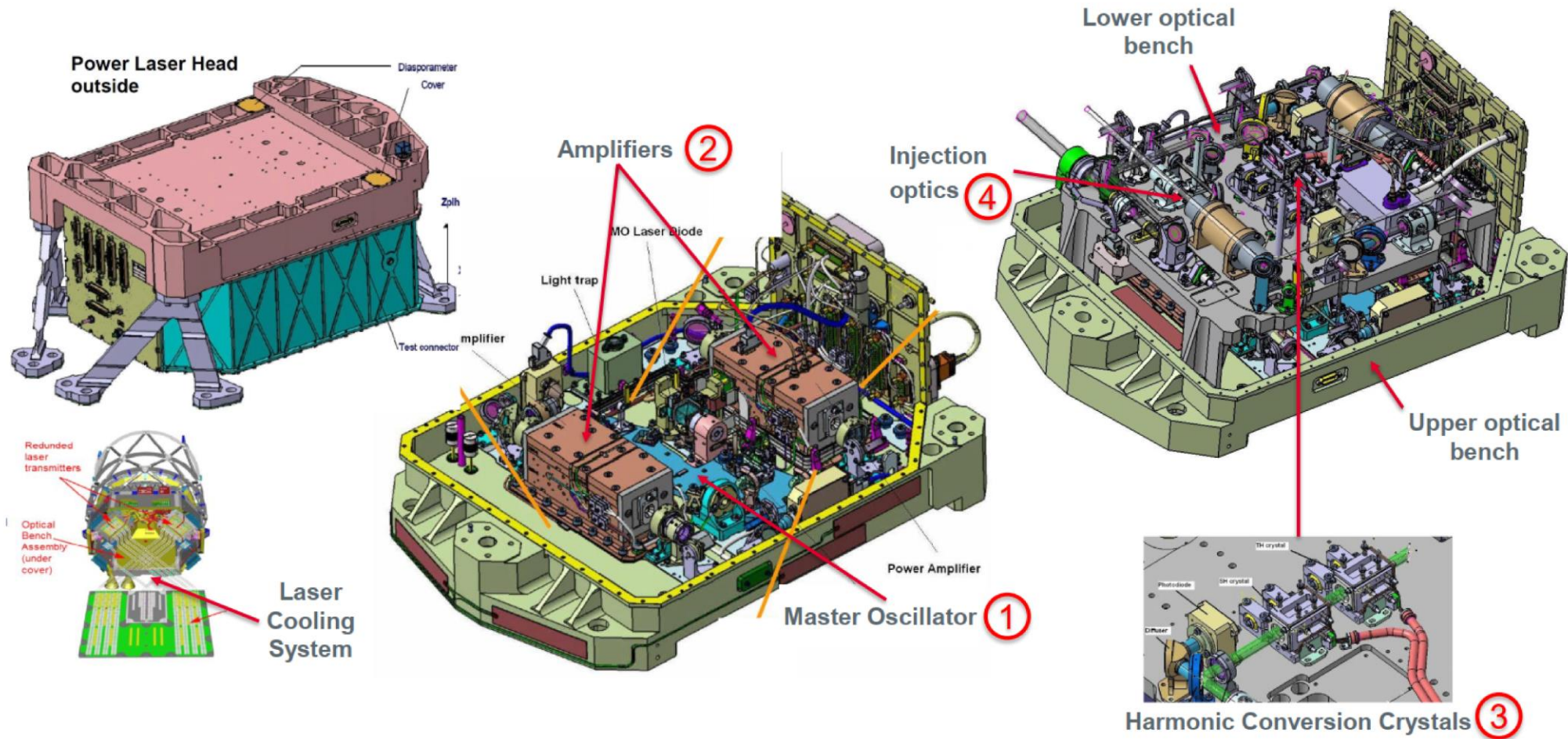


- **Injection-seeded and frequency-tripled master oscillator power amplifier Nd:YAG system** at 355 nm wavelength, manufactured by *Leonardo*
- **Monitoring of the laser status and performance** based on photodiodes, temp. sensors, receiver raw data
- **Strong expertise gained from airborne demonstrator** to support laser activities, anomaly investigations, etc.



Parameter	Value
Type	Frequency-tripled Nd:YAG
Laser wavelength	354.8 nm
Pulse repetition rate	50.5 Hz
Pulse energy (measured with PD74)	FM-A: 40 to 70 mJ; FM-B: 60 to 100 mJ (182 mJ over 1 day)
Pulse energy correction factors for PD74	FM-A: 0.7663; FM-B: 0.9409
Pulse width (FWHM)	20 ns
Spectral width (FWHM)	< 50 MHz
Frequency stability (rms over 540 pulses)	< 12 MHz (< 7 MHz at optimized cavity control setting)
Beam diameter	< 6.2 mm
Beam divergence (full angle)	< 600 μ rad
Operation time in space	FM-A: 15 months; FM-B: 41 months
Total number of pulses	FM-A: 1.9 Gigashots; FM-B: 5.3 Gigashots

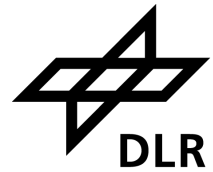
Optical design of the laser transmitter



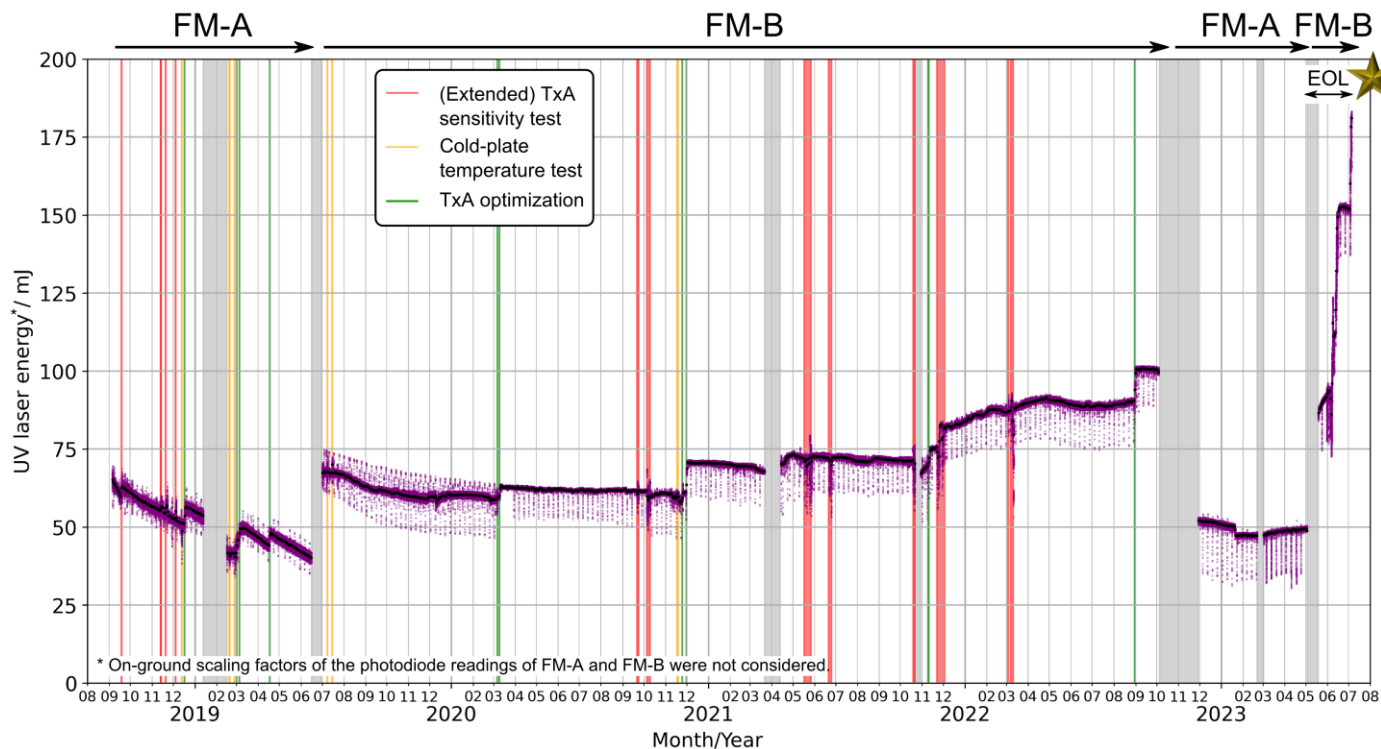
Figs. courtesy of V. De Sanctis (Leonardo)

- The power laser head was composed of an *upper optical bench* in direct contact with the thermal interface plate, carrying all the active (dissipating) components, whereas passive components were located on a separated *lower optical bench*
- Mitigation of laser-induced contamination by **in-situ cleaning system** using low pressures of oxygen, was not fully consumed

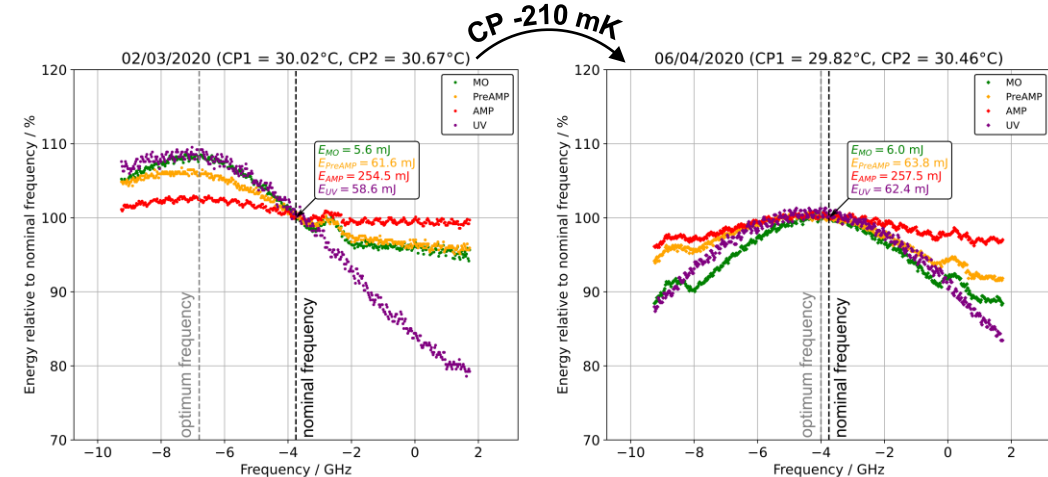
UV energy evolution, relationship with laser temperatures



- **Strong energy decrease during first FM-A phase** (Sep 18 – Jun 19) due to operation at non-optimal cold-plate temperature (CP-T) setpoint.
- Optimization of thermal setpoint for FM-B in Mar 20 led to **stable laser operation for over 40 months** during which energy was incrementally increased to 100 mJ to compensate for the signal loss on the emit path.
- Following the switch-back to FM-A in Nov 2022, the **gained insights into the interplay of temperature, frequency, and laser energy** enabled the stabilization of FM-A's performance at around 50 mJ.

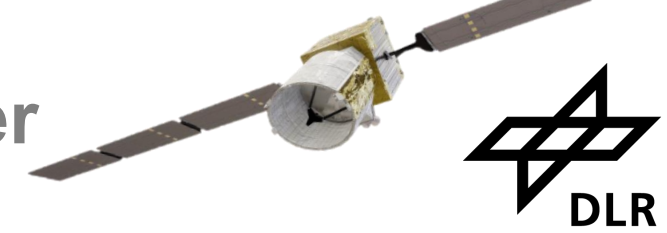


Energy vs. frequency (FM-B)



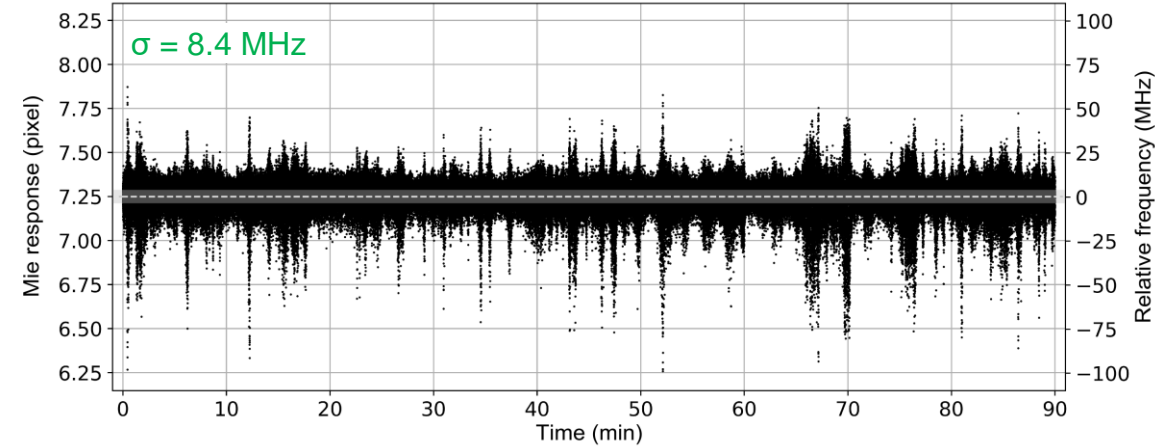
- **Laser settings were varied during (extended) sensitivity tests (13), temperature tests (7) and laser optimizations with permanent changes (12).**
- **3 laser switches** in 2019, 2022 and 2023 and **4 Failure Detection, Isolation and Recovery (FDIR)** events interrupted the laser operation; duration of switch-on procedure was strongly reduced from one month to six days.
- During the final **33 hours** before the final switch-off, the **laser was operated at 182 mJ!**

Impact of satellite's reaction wheels on the laser frequency stability

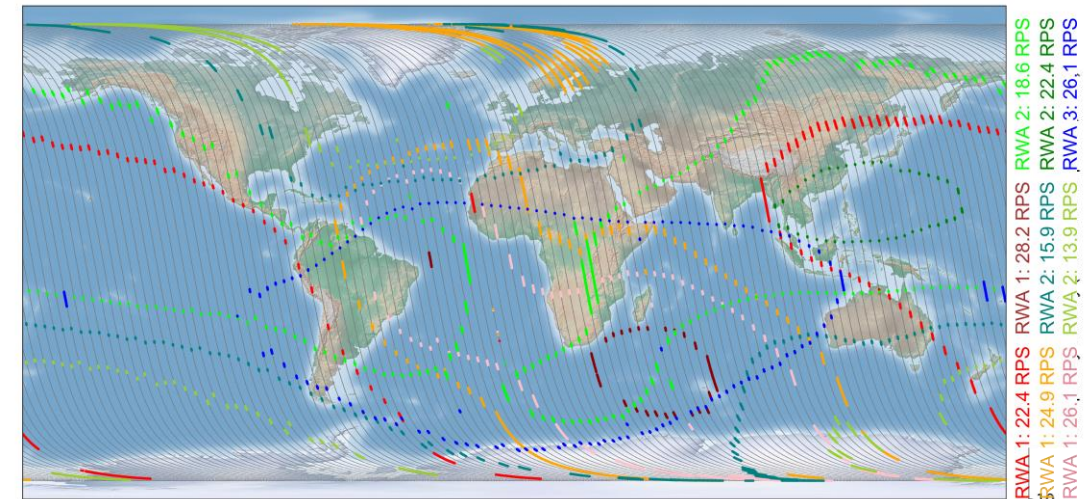


- **Overall good frequency stability** (8-10 MHz shot-to-shot, rms), but periods of increased noise (tens of seconds) with $\sigma > 15$ MHz.
- **Frequency noise depended on the geolocation of the satellite**, as it was enhanced at specific rotation speeds of **the three reaction wheels**, suggesting that **micro-vibrations** were the root cause.
- Enhanced frequency noise had **only minor impact on the global Rayleigh and Mie wind errors** (< 0.1 m/s) and ground velocities, as the portion of affected observations was “only” 10 to 20%.
- When utilizing Aeolus data on smaller geographical scales, the **geolocational dependence of the frequency stability should be considered** (e.g. ground station validation).

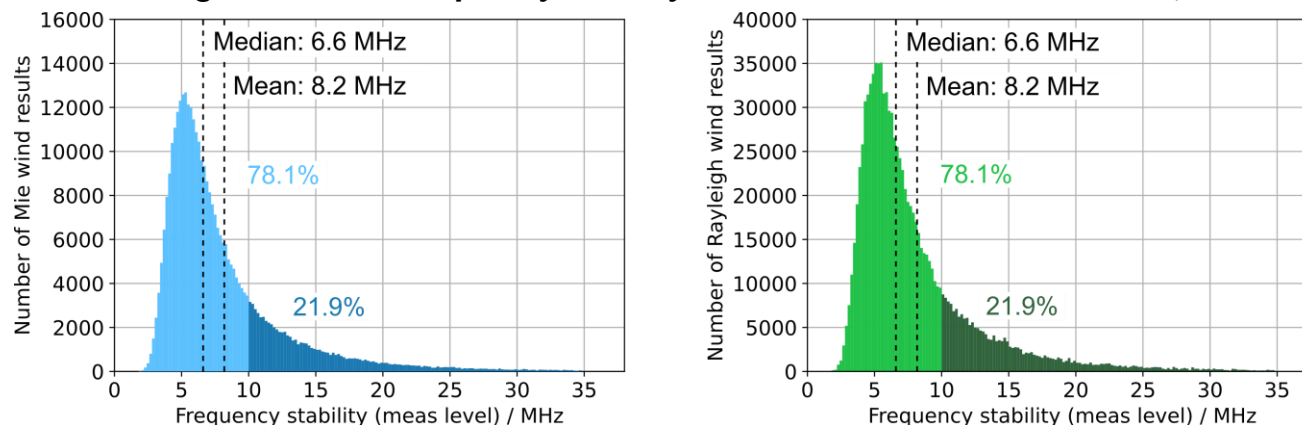
Laser frequency stability over one orbit on 14/10/2019



Observations with increased frequency noise in CW 47, 2019

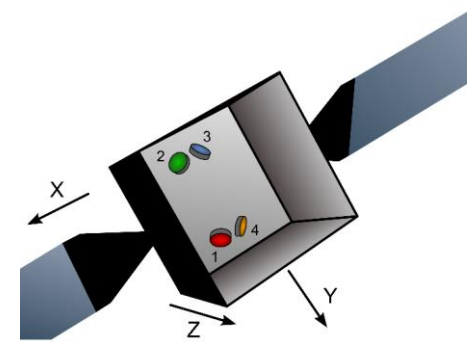
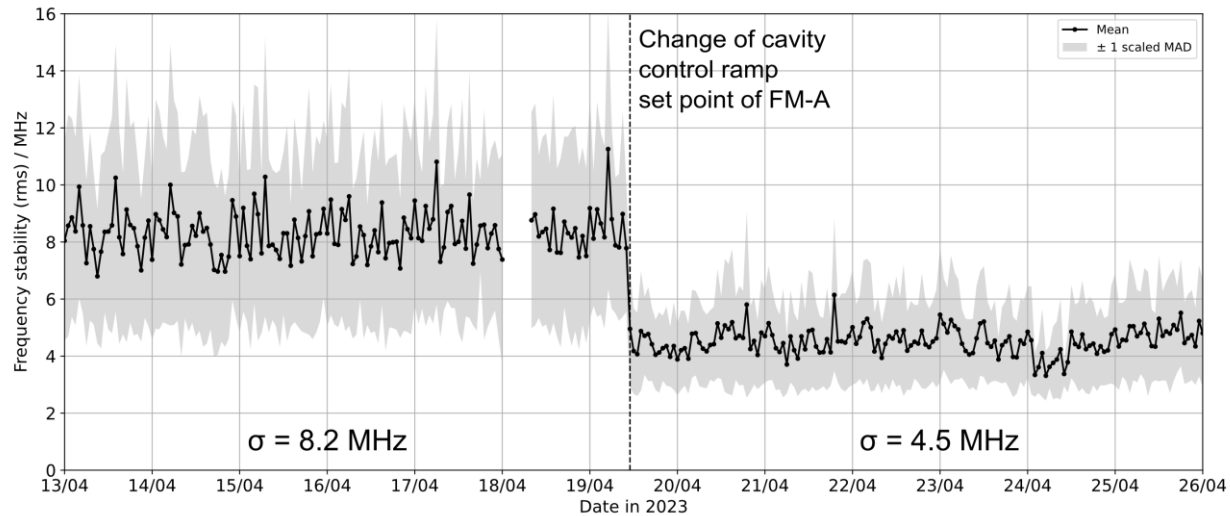


Histogram of laser frequency stability on measurement level in CW 34, 2020



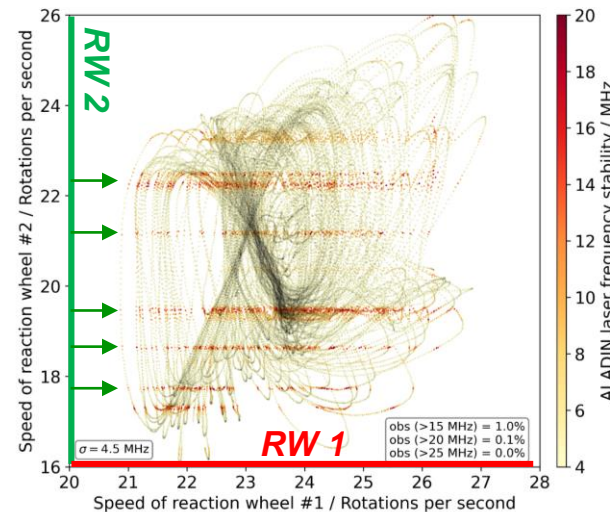
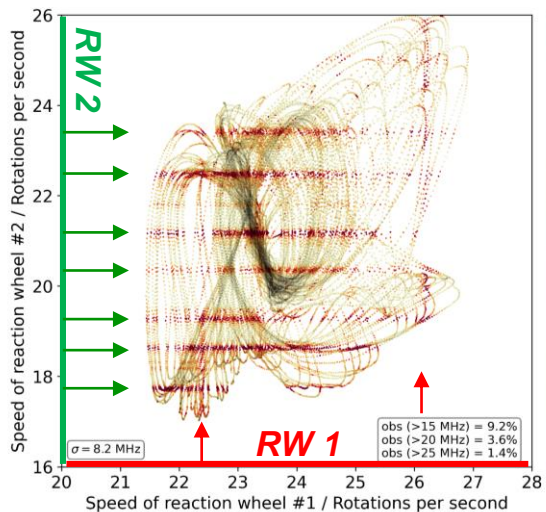
Enhancing the frequency stability during end-of-life tests

Laser frequency stability and correlation with reaction wheel speeds before and after optimization of the cavity control setting



Orientation of the four reaction wheels with respect to the spacecraft body.

- As one of the **end-of-life activities**, the **master oscillator cavity length stabilization was modified** (change of ramp set point in ramp-hold-fire technique).
- The setting change **greatly improved the frequency stability by a factor of two for both lasers**.
- In particular, the **influence of micro-vibrations from the reaction wheels was largely diminished**, thereby reducing the portion of observations with degraded stability ($\sigma > 15$ MHz) from up to 20% to only 1.0%.
- However, comparison of the wind data against the ECMWF model from M. Rennie **did not show any improvement in the random errors**.





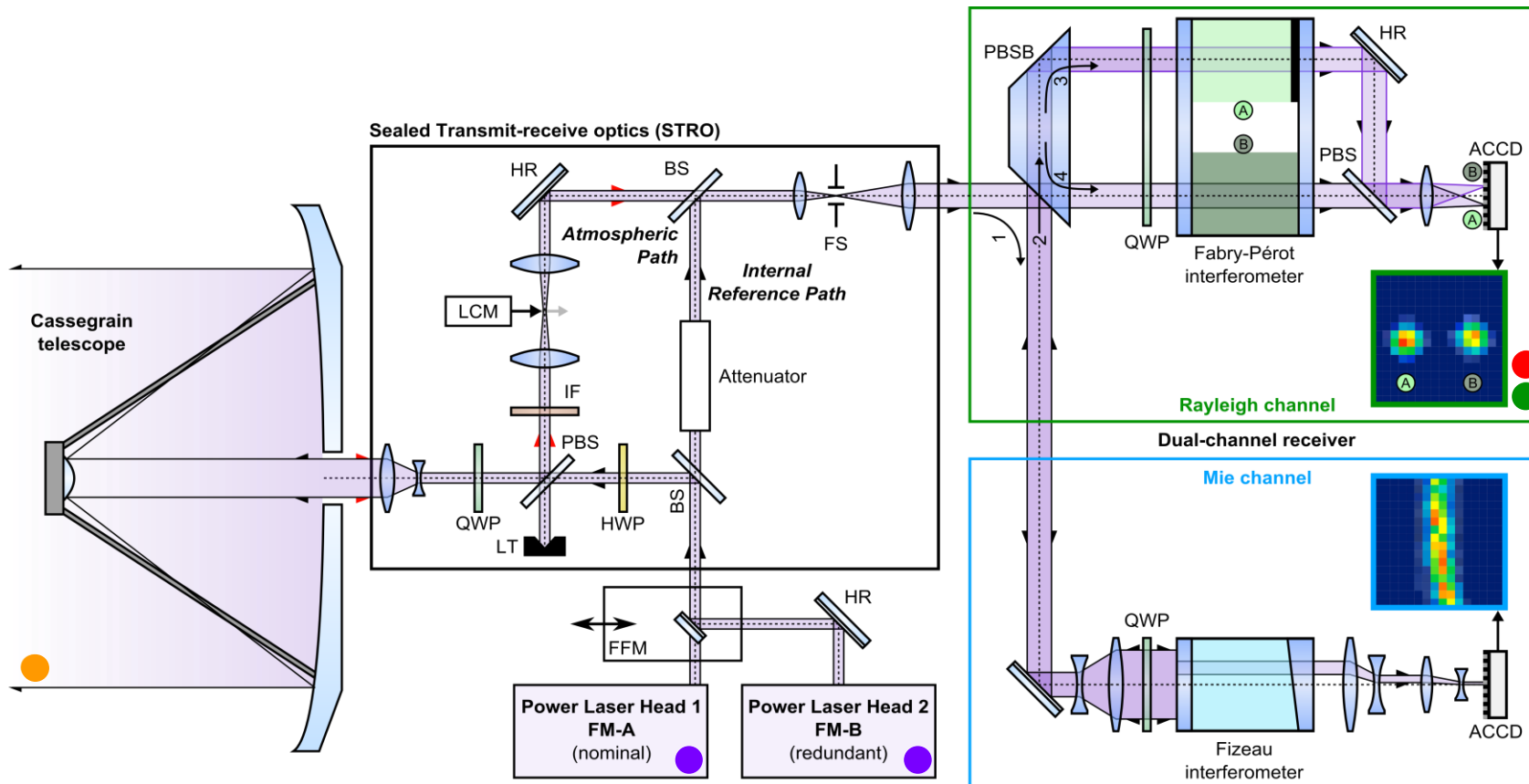
RECEIVER SIGNAL EVOLUTION

Measurement of the ALADIN signal levels

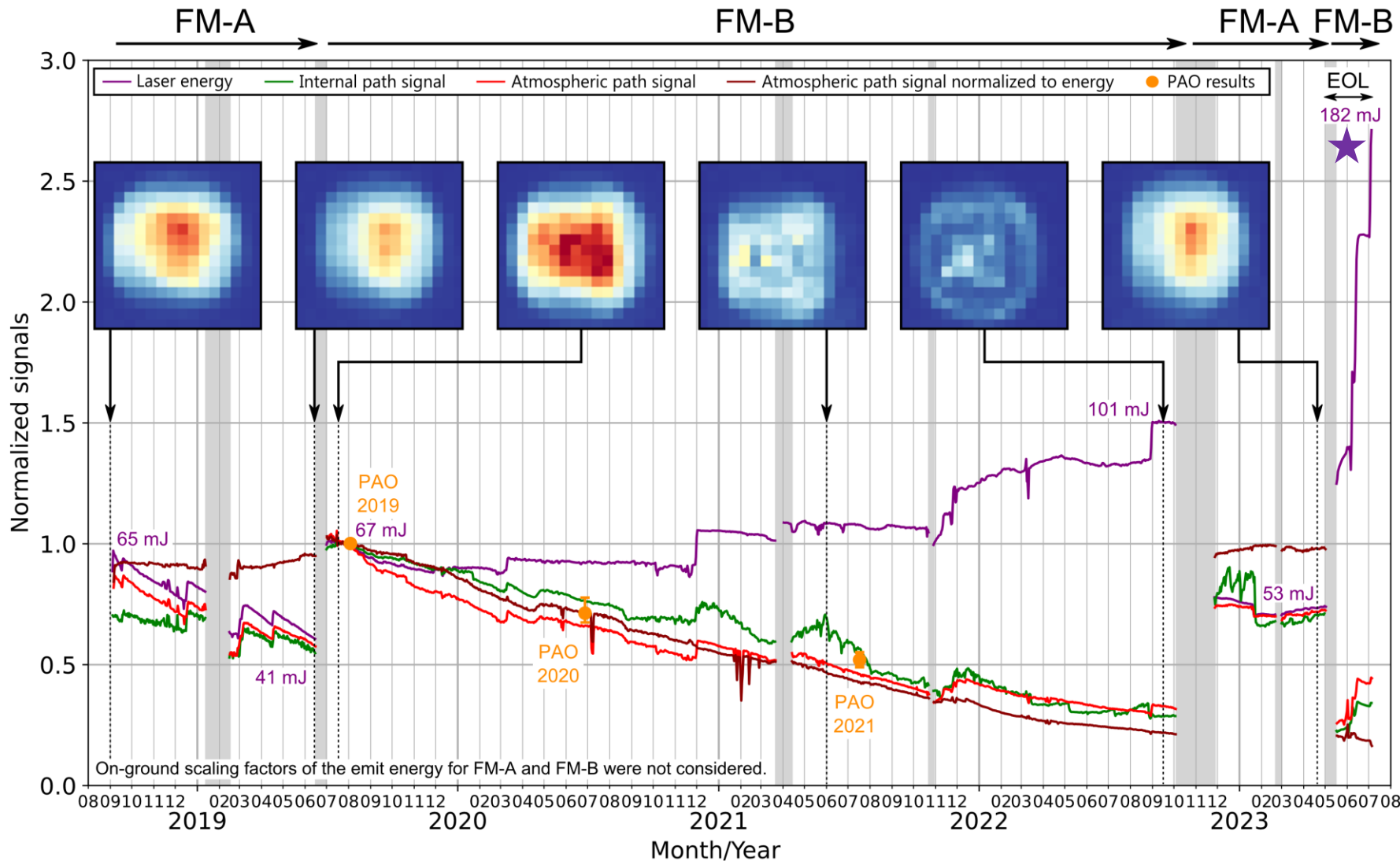
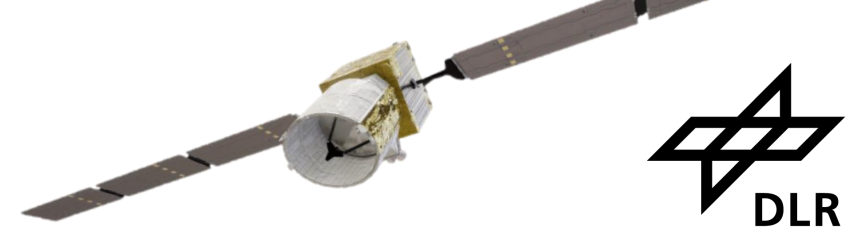


- Precise quantification of the ALADIN signal performance was crucial, as it determined the wind random error, particularly for the Rayleigh channel ($\sigma \propto 1/\sqrt{ATM}$).
- Signal evolution was carefully monitored based on housekeeping and Aeolus detector data.
- Methods and programming tools were developed and refined over the mission.
- Monitoring of the instrument performance has driven decision-making processes (switch to FM-A) and supported special operations (laser tests, optimizations, end-of-life activities).

- **Laser-internal photodiodes** for energy monitoring at different stages of the laser system (master oscillator, amplifiers, harmonic section), available at 0.25 Hz sampling rate
- **Internal reference signal (INT)** (small portion of the laser emission directly guided to the field stop) for measurement of the outgoing laser frequency, receiver calibration modes and laser beam monitoring (LBM), available on single pulse level (50.5 Hz)
- **Atmospheric return signal (ATM)** (collected from the telescope) for retrieving Doppler shift and backscatter information, available on measurement level (0.4 Hz to 2.5 Hz depending on operational settings)
- **Pierre Auger observations (PAO)** (on-ground cosmic ray observatory) to estimate laser energy at the output of the telescope, available on a few days between 2019 and 2021



Signal evolution over the mission period



- The **signal levels dropped by about 40% during the first 8 months of the mission**, almost entirely due to energy loss in the FM-A master oscillator.
- **FM-B was operating for more than 3 years with a UV loss of only 25%** considering pump current increases, which is in line with the best-case lifetime degradation expectations.
- However, **considerable signal loss (-70%) was evident in the internal and emit path**, verified by on-ground measurements (Pierre Auger Obs.)
- **Switchback to FM-A in October 2022 restored the transmission from 2019**, increased the ATM signal levels by 120% despite lower laser energy.
- **FM-A energy was stable** until end of nominal operations on 30 April 2023 thanks to optimized thermal conditions.
- In the frame of the **end-of-life activities, FM-B was activated again** and almost scaled to its maximum output energy, which was, however, not fully transmitted to the INT and ATM path.

A composite image showing a satellite in space with a purple beam of light directed towards a building on the ground at night. The sky is filled with stars and the Milky Way. The ground is dark with some structures and a small light source on the horizon.

MEASUREMENTS AT THE PIERRE AUGER OBSERVATORY

Observing ALADIN's UV laser beam on ground

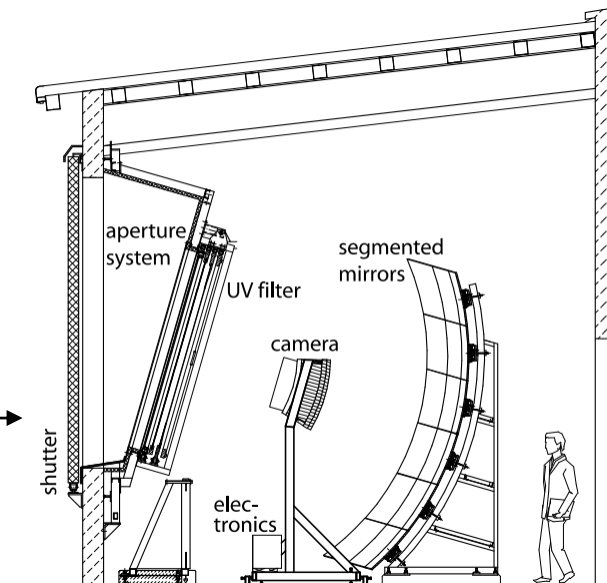
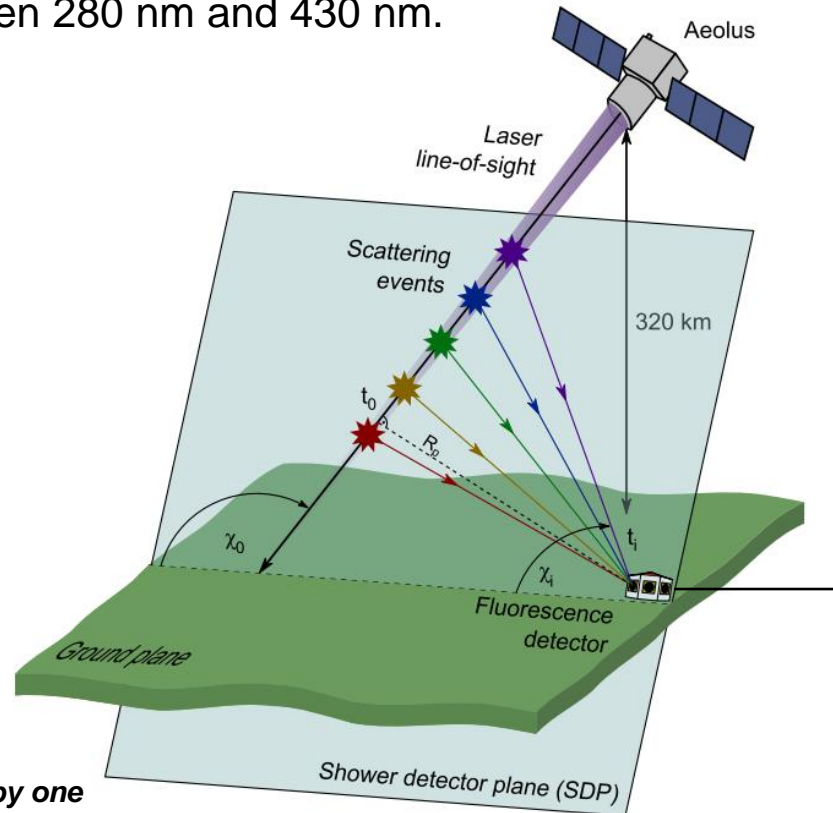


- First measurements of a space-borne ultraviolet laser beam by an Earth-based cosmic ray observatory.
- Pierre Auger Observatory is the world's leading experiment for measuring ultra-high-energy cosmic radiation in the Earth's atmosphere.
- One method is fluorescence detection in the UV wavelength range between 280 nm and 430 nm.



The Pierre Auger Collaboration et al.,
Optica, 11, 263 (2024).

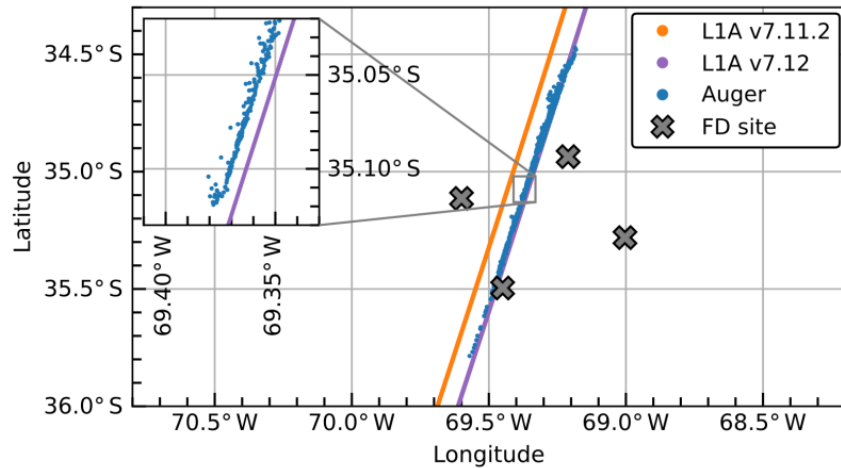
- **ALADIN laser beam was visible once a week during SH winters** when passing the observatory in Argentina which consists of 4 sites with 6 fluorescence detectors each.
- **Geometrical reconstruction of the laser beam** after being scattered by molecules when passing through the atmosphere (similar to fluorescent light from cosmic-ray air showers).



Structure of one fluorescence detector telescope of the Pierre Auger Observatory

Geometry of the Aeolus laser beam being detected by one of the four fluorescence detectors of the Pierre Auger Observatory

Ground-truth verification of geolocation and laser energy

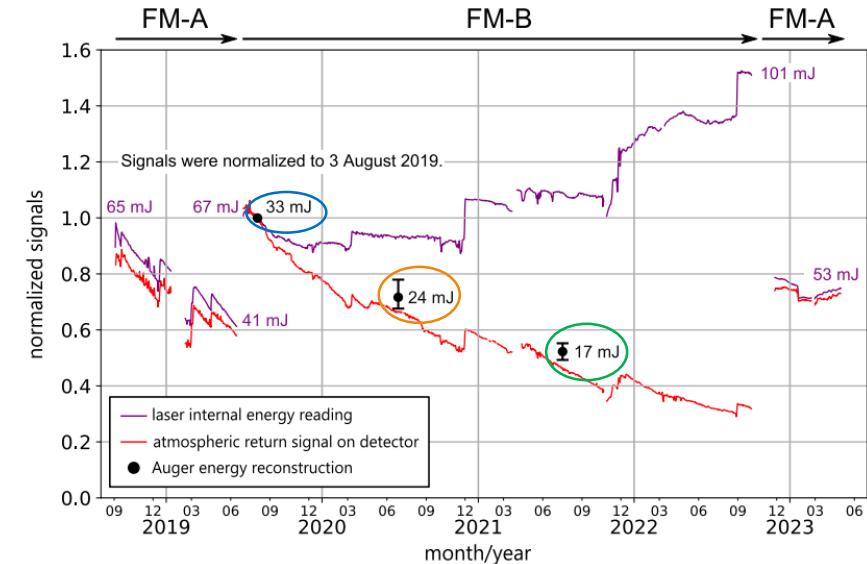
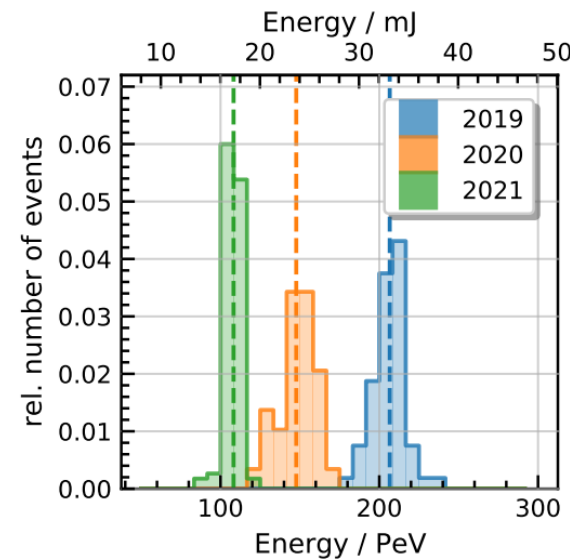


Geolocation derived with different Aeolus data processor versions before (orange) and after (purple) of the error correction and measurements by the Auger Observatory (blue dots) at 10 km altitude for the overpass on 17/07/21.

- Confirmation that signal is already lost between the laser output and the telescope
- Reconstructed energy at FM-B start (33 mJ) is lower than expected at telescope output when considering emit path transmission (44 mJ)

→ **Precedent for the performance verification of EarthCARE and Aeolus-2**

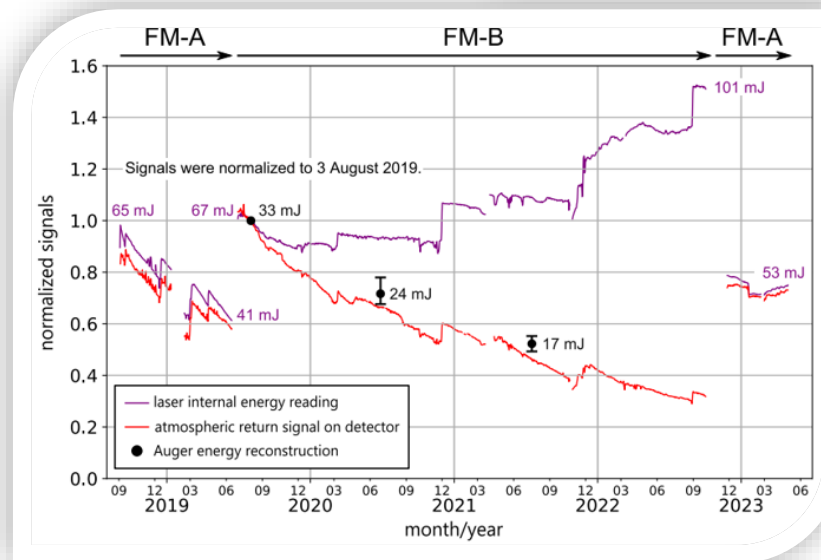
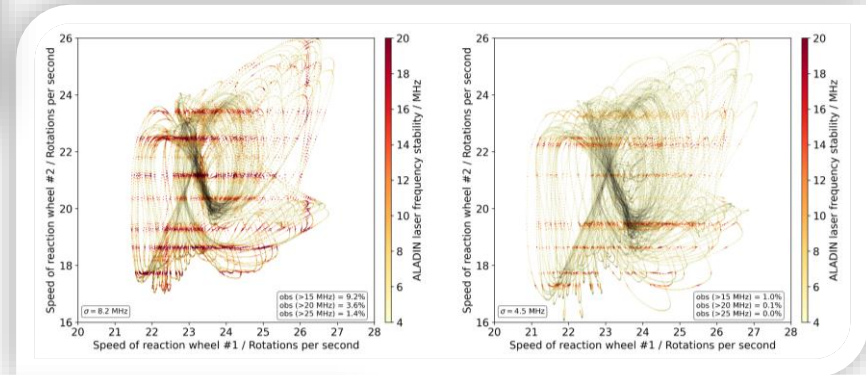
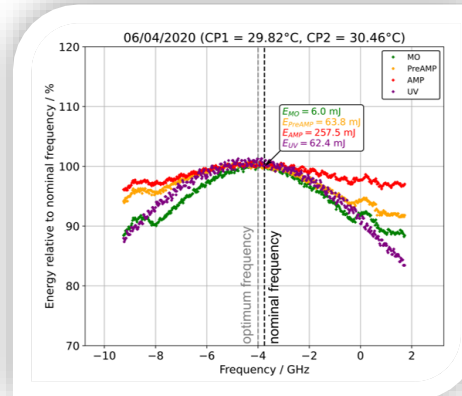
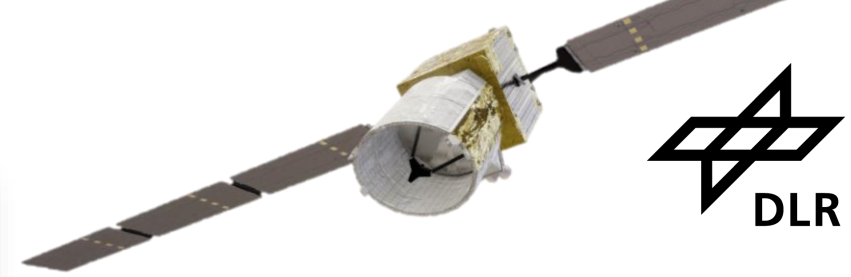
- Support of the Aeolus mission by providing valuable information on both instrument and satellite performance:
 1. **Accurate determination of the laser beam ground track**
 2. **Independent measurement of the emitted laser energy**
- Correction of an error in the Aeolus processor to reduce the offset between the assumed and the measured ground track from 6.8 km to 0.8 km



Left: Reconstructed energies for three Aeolus overpasses during the FM-B period from 2019 to 2021. Right: Signal evolution of the laser energy (purple line), the atmospheric return signal under clear-air conditions (red line) and the Auger measurements (black dots).

Summary and conclusions

- The **Aeolus mission was a groundbreaking achievement in Earth observation and space laser technology**, demonstrating the successful operation of UV high-power lasers in orbit over almost five years (>7.2 Gshots for FM-A, FM-B).
- After **optimization of the thermal settings**, **both laser provided stable output up to 100 mJ** (182 mJ during the final 33 hours before switch-off).
- The **laser frequency stability was affected by micro-vibrations** at specific rotation frequencies of the satellite's reaction wheels, but could be **improved by a factor of 2** through an adjustment of the cavity control settings to **meet the system requirement of <7 MHz (rms)**.
- **Strong signal loss** by 70% between 2019 and 2022 was caused by laser-induced contamination and/or damage on the optics that guide the redundant laser output onto the common emission path.
- The root cause analysis of the signal loss was supported by **energy measurements at the PAO** which **set a precedent for the ground-truth verification of EarthCARE and Aeolus-2**.



A satellite with two large solar panel arrays is shown in orbit above the Earth. The satellite is white with a complex structure and is positioned centrally in the upper half of the frame. The solar panels are extended horizontally to the left and right. The Earth's surface is visible below, showing a mix of blue oceans, green landmasses, and white cloud formations. The horizon of the Earth is a clear, curved line separating the planet from the blackness of space.

THANK YOU FOR YOUR ATTENTION!